J Mol Model (2012) 18:1625–1632
DOI 10.1007/s00894-011-1183-4

ORIGINAL PAPER

# A theoretical study on the hydrolysis mechanism of carbon disulfide

**Lixia Ling · Riguang Zhang · Peide Han · Baojun Wang**

Received: 30 November 2010 / Accepted: 7 July 2011 / Published online: 30 July 2011

**Abstract** The hydrolysis mechanism of $CS_2$ was studied using density functional theory. By analyzing the structures of the reactant, transition states, intermediates, and products, it can be concluded that the hydrolysis of $CS_2$ occurs via two mechanisms, one of which is a two-step mechanism ($CS_2$ first reacts with an $H_2O$, leading to the formation of the intermediate COS, then COS reacts with another $H_2O$, resulting in the formation of $H_2S$ and $CO_2$). The other is a one-step mechanism, where $CS_2$ reacts with two $H_2O$ molecules continuously, leading to the formation of $H_2S$ and $CO_2$. By analyzing the thermodynamics and the change in the kinetic function, it can be concluded that the rate-determining step involves H and OH in $H_2O$ attacking S and C in $CS_2$, respectively, causing the C=S double bond to change into a single bond. The two mechanisms are competitive. When performing the hydrolysis of $CS_2$ with a catalyst, the optimal temperature is below 252°C.

**Keywords** Carbon disulfide · Hydrolysis mechanism · DFT · Quantum chemistry calculation

## Introduction

$CS_2$ is a sulfur-containing organic compound that is often found in Claus tail gas, petroleum, natural gas, and various raw gases made from coal [1, 2]. Trace levels of $CS_2$ affects the environment and leads to economic problems within processes downstream, such as the syntheses of methanol, ammonia and urea. The detrimental effect that sulfur has upon many catalysts has been well documented [3]. Apart from affecting catalysts, the presence of sulfur can also lead to increased corrosion of the reactors used in refining processes [4]. The need to remove $CS_2$ has become increasingly important, and some technologies—including catalytic hydrolysis, oxidation conversion, and hydrogenation conversion [5–9]—have been developed to remove $CS_2$. Attention has recently focused on the hydrolysis of $CS_2$ due to the mild reaction conditions and relatively few side reactions involved, as well as the fact that it is inexpensive [10]. Zou et al. [11] studied the hydrolysis of $CS_2$, and found that the equilibrium constant for this hydrolysis $\log K_{CS2}$ is 12.0740 at 100 °C, but only 4.5314 at 600 °C. It is thus apparent that using a suitable temperature range is key to optimizing the conversion rate during $CS_2$ hydrolysis.

In addition, the kinetics of $CS_2$ hydrolysis is considered to be more complicated than the hydrolysis of another sulfur-containing organic compound, COS [6], so it is necessary to investigate the process of $CS_2$ hydrolysis in detail. Up to now, there have been some experimental

---

L. Ling
Research Institute of Special Chemicals,
Taiyuan University of Technology,
Taiyuan 030024 Shanxi, People's Republic of China

L. Ling · P. Han
College of Materials Science and Engineering,
Taiyuan University of Technology,
Taiyuan 030024 Shanxi, People's Republic of China

R. Zhang · B. Wang (✉)
Key Laboratory of Coal Science and Technology,
Ministry of Education and Shanxi Province,
Taiyuan University of Technology,
Taiyuan 030024 Shanxi, China
e-mail: wangbaojun@tyut.edu.cn

studies on the mechanism of $CS_2$ hydrolysis. Shangguang et al. [12] investigated the hydrolysis of $CS_2$, and noted both a two-step and a one-step mechanism, as shown in reactions (1) and (2) below, respectively:

$$\begin{aligned} &CS_2 + H_2O \rightarrow COS + H_2S \\ &COS + H_2O \rightarrow CO_2 + H_2S \end{aligned} \tag{1}$$

$$CS_2 + 2H_2O \rightarrow 2H_2S + CO_2. \tag{2}$$

While $CS_2$ hydrolysis involves these two mechanisms, they found that the hydrolysis of $CS_2$ to $H_2S$ and $CO_2$, not via the intermediate COS, is the major reaction according to mathematical analysis and experimental data fitting. However, other researchers have different opinions in this regard. $CS_2$ hydrolysis has been studied by analyzing the sulfur-containing compounds in tail gas by Wang et al. [13], and it was confirmed that $CS_2$ hydrolysis first gives rise to COS, then COS hydrolyzes via hydrogen thiocarbonate, leading to the formation of $H_2S$. In this process, the hydrolysis of $CS_2$ to COS is the rate-determining step, while COS to $H_2S$ is a fast reaction. This result was backed by Laperdrix et al. [14] and Sahibed-Dine et al. [15], who studied the process of $CS_2$ hydrolysis using IR. Tong et al. [6] studied the kinetics of $CS_2$ hydrolysis, and their results agreed with the two-step mechanism mentioned above. Thus, the predominant mechanism for $CS_2$ hydrolysis remains unknown. With the development of quantum chemistry, density functional theory (DFT) has proven capable of providing qualitative and quantitative insights into reaction mechanisms [16]. The addition of OH radicals to $CS_2$, and the saddle points for conversion of $CS_2$ to COS, which ultimately leads to the formation of $SO_2$, have been calculated at the modified G1 level of theory, and it was found that the addition of OH to a sulfur atom is more favorable than its addition to the carbon atom of $CS_2$ [17]. A theoretical study of the adduct $H+CS_2$ has been reported by Bohn et al. [18]. The major product in the reaction of H atoms with $CS_2$ has been identified as *trans*-HSCS from the matrix infrared spectrum and ab initio calculations of structure and the infrared spectrum. The reaction of N and $CS_2$ was studied using DFT at the B3LYP (full)/6-311+G** and CCSD (T)/6-311+G* levels of theory by Wang et al. [19]. The results showed that the reaction channel $N+CS_2 \rightarrow CS+NS$ is easily achieved because of its low energy barrier, which is in agreement with experimental observations. Zheng et al. [20] also investigated the reaction mechanism of the reaction of O ($^3P$) with $CS_2$ using DFT at the B3LYP/6-311++G(d, p) level of theory. It was concluded that the products of the reaction of $CS_2+O(^3P)$ are CS and SO, in good agreement with experimental observations. Recently, the water-catalyzed hydrolysis reaction of $CS_2$ in aqueous solution ($\varepsilon$=78.4) has been investigated at the levels of HF and MP2 with the 6-311++G(d, p) basis set using the polarizable continuum model (PCM), and the activation Gibbs free energies in water solution for the rate-determining steps of 1–6 hydrolysis processes were obtained by Deng et al. [21]. The hydrolysis of COS was also studied by Deng et al. [22].

In the study described in this paper, the two mechanisms of $CS_2$ hydrolysis leading to the formation of $H_2S$ and $CO_2$ were studied using DFT. The main aims of our study were (i) to find the most favorable path for the hydrolysis of $CS_2$ by analyzing the microscopic structural parameters, the change in the thermodynamic function, and the change in the kinetic function, and (ii) to obtain the optimal temperature range for $CS_2$ hydrolysis.

## Computational methods

A DFT method was adopted and calculations were performed using the Dmol$^3$ program [23] running in the Materials Studio 4.0 package. The reactant, intermediates and products were optimized at the level of the generalized gradient approximation (GGA) using the Perdew–Wang 1991 (PW91) functional [24] and DND basis set. Unrestricted spin was chosen, the total SCF tolerance criteria, integration accuracy criteria and orbital cutoff quality criteria were set at medium, and multipolar expansion was set to octupole. TS search calculations were then carried out to find a possible transition state structure for each elementary reaction using the LST/QST method. All of the structures were calculated at the same level of theory, and vibration analysis was carried out for each structure to characterize it as either an equilibrium structure (no imaginary frequency) or a transition state (one imaginary frequency whose vibrational mode corresponds to the reaction coordinate). Meanwhile, the electronic energy ($E_{\text{elec}}$) and zero-point vibration energies (ZPVE) were calculated. TS confirmation calculations were carried out using the NEB method to confirm that every transition state leads to the desired reactant and product. All calculations were performed on a Dell Pentium D PC server system.

In order to evaluate the reliability of the selected calculation method and parameters, the bond lengths and bond angles of three sulfur-containing molecules were calculated, and the calculated and experimental results [25] are shown in Table 1. The calculated results are in agreement with the experimental structural parameters, the largest deviation in the bond angles is 1.323°, and the deviation in the bond lengths is smaller than 0.0254 Å. In addition, some results relating to the reaction mechanism were obtained using the above method and parameters in

**Table 1** Calculated and experimental bond lengths (Å) and bond angles (°) of COS, $CS_2$ and $H_2S$

| COS | | | | | | $CS_2$ | | | | $H_2S$ | | | |
|---|---|---|---|---|---|---|---|---|---|---|---|---|---|
| C—O | | C—S | | ∠ O—C—S | | C—S | | ∠ S—C—S | | H—S | | ∠ H—S—H | |
| $L_{cal}$ | $L_{exp}$ | $L_{cal}$ | $L_{exp}$ | $A_{cal}$ | $A_{exp}$ | $L_{cal}$ | $L_{exp}$ | $A_{cal}$ | $A_{exp}$ | $L_{cal}$ | $L_{exp}$ | $A_{cal}$ | $A_{exp}$ |
| 1.1730 | 1.1578 | 1.5720 | 1.5601 | 179.927 | 180.000 | 1.5660 | 1.5526 | 180.000 | 180.000 | 1.3610 | 1.3356 | 90.797 | 92.120 |

our previous studies [26–28]. At the same time, the bigger basis set, DNP, which is equivalent in accuracy to the 6-31G** Gaussian orbital basis set, was used to calculate the step IM1→IM2 (see Fig. 1). The results show that the activation energy is 168.04 kJ $mol^{-1}$ with the DND basis set, and 169.01 kJ $mol^{-1}$ with DNP basis set. The rate constants are −45.19 $s^{-1}$ and −47.14 $s^{-1}$, respectively. This indicates that the DND basis set can meet the requirements of the calculation.

## Results and discussion

### Reaction mechanism

The two-step mechanism and one-step mechanism for $CS_2$ hydrolysis (reactions (1) and (2), respectively) are shown in Fig. 1, the optimized geometries for the reactants, intermediates, transition states, products and their atomic numbers along the reaction pathways are shown schematically in Fig. 2, and the imaginary frequency of each transition state and the bonds corresponding to relative normal vibrations during the process of $CS_2$ hydrolysis are shown in Table 2.

In the two-step mechanism of $CS_2$ hydrolysis, first $CS_2$ reacts with an $H_2O$ molecule, leading to IM1. IM1 is the reactant-like intermediate in which two reactant molecules interact with each other by van der Waals forces of strength 7.49 kJ $mol^{-1}$, and their geometries remain almost the same as the corresponding free molecules. Then, H and OH in $H_2O$ attack S and C atoms in $CS_2$, respectively, and the attacked double bond in $CS_2$ changes into a single bond. The original linear $CS_2$ molecule is thus distorted, and a hydrogen dithiocarbonate species IM2 is formed via TS1. TS1 has one imaginary frequency of −1290.68 $cm^{-1}$, corresponding to the stretch mode of O1–C5 and the migration of H3 from O1 to S4. Subsequently, H2 migrates from O1 to S4, leading to the formation of by-product IM3. The bond length of S4–C5 in IM3 is 3.667 Å, which shows that $H_2S$ separates from the original structure and COS is

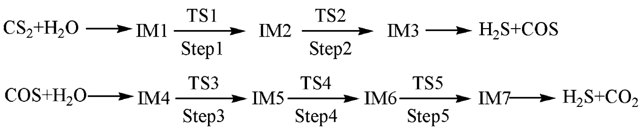

Two-step mechanism

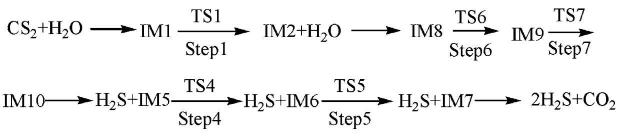

One-step mechanism

**Fig. 1** Mechanisms for the hydrolysis of $CS_2$

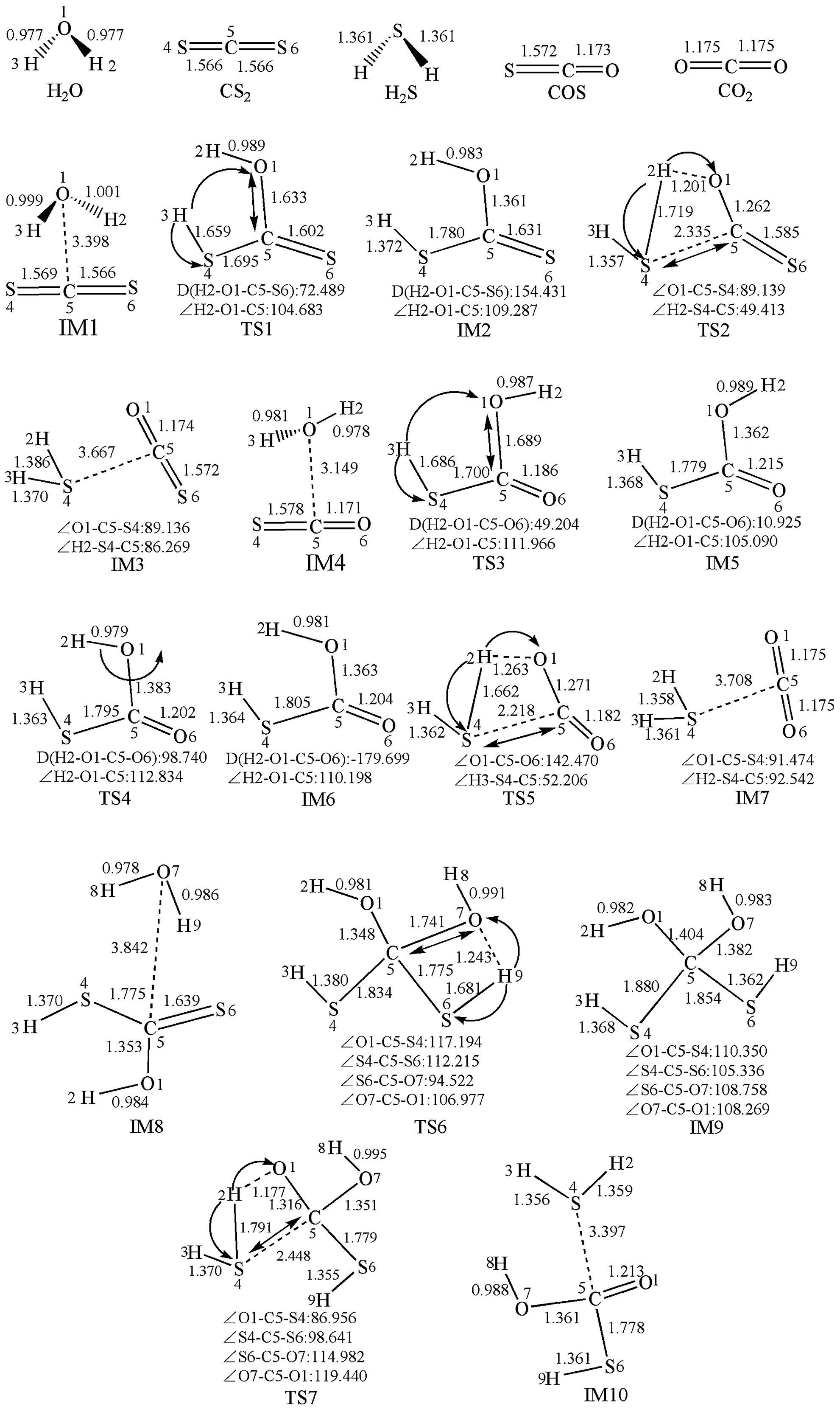

**Fig. 2** Optimized geometries for various species involved in the hydrolysis of $CS_2$

formed. The two product molecules, $H_2S$ and COS, interact with each other by van der Waals forces of strength 0.62 kJ mol$^{-1}$, and their geometries remain almost the same as those for the corresponding free molecules. The

**Table 2** Imaginary frequency of each transition state and the bonds corresponding to relative normal vibrations

| Transition state | Imaginary frequency ($cm^{-1}$) | Bonds corresponding to normal vibrations |
|---|---|---|
| TS1 | −1290.68 | H3–O1–S4; O1–C5 |
| TS2 | −1342.31 | H2–O1–S4; S4–C5 |
| TS3 | −1367.93 | H3–O1–S4; O1–C5 |
| TS4 | −616.76 | H2–O1–C5 |
| TS5 | −1407.03 | H2–O1–S4; S4–C5 |
| TS6 | −1268.34 | H9–O7–S6; C5–O7 |
| TS7 | −1258.29 | H2–O1–S4; C5–S4 |

corresponding transition state TS2 has a four-membered ring (H2–S4–C5–O1), which has one imaginary frequency of −1342.31 $cm^{-1}$ due to the stretch mode of S4–C5 and the migration of H2 from O1 to S4.

Next, COS is hydrolyzed by another $H_2O$ molecule, resulting in the reactant-like intermediate IM4, in which there is an interaction energy of 7.10 kJ $mol^{-1}$ between COS and $H_2O$. H and OH in $H_2O$ attack the S and C atoms in COS, respectively, leading to the formation of a hydrogen thiocarbonate species IM5. The bond lengths of O1–C5 and H3–S4 are 1.362 Å and 1.368 Å, respectively. In step 4, IM5 then isomerizes to IM6; it can be seen in Fig. 2 that H2 is deflected, causing the dihedral angle H2–O1–C5–O6 to change from 10.925° to −179.699°. Finally, H2 migrates from O1 to S4, leading to the formation of by-product IM7 via TS5, which has one imaginary frequency of −1407.03 $cm^{-1}$ corresponding to the stretch mode of S4–C5 and the migration of H2 from O1 to S4. In IM7, $H_2S$ and $CO_2$ are formed, and there is an interaction energy of 11.10 kJ $mol^{-1}$ between $H_2S$ and $H_2O$.

The one-step mechanism has the same steps as the two-step mechanism from reactants to IM2. IM2 then reacts with another $H_2O$ molecule, initially producing IM8, in which there is an interaction energy of 30.16 kJ $mol^{-1}$ between the two molecules. H and OH in $H_2O$ then attack the S6 and C5 atoms in IM2, respectively, leading to the formation of a tetrahedral intermediate, IM9, in which the angles O1–C5–S4, S4–C5–S6, S6–C5–O7 and O7–C5–O1 are 110.350°, 105.336°, 108.758° and 108.269°, respectively (similar to the angle H–C–H in $CH_4$). Subsequently, H2 in IM9 migrates from O1 to S4 via TS7, which has one imaginary frequency of −1258.29 $cm^{-1}$ corresponding to the stretch mode of S4–C5 and the migration of H2 from O1 to S4. Meanwhile, an $H_2S$ molecule separates from the original structure, a similar structure to IM5 is formed, and there is an interaction energy of 6.81 kJ $mol^{-1}$ between the two molecules. The similar structure to IM5 is then optimized, resulting in IM5 itself. From IM5 to the final products $CO_2$ and $H_2S$, the one-step mechanism exhibits the same steps as the two-step mechanism.

In these two mechanisms, H migration occurs in every step. There are two types of H migration: intermolecular H migration (for example, H in $H_2O$ migrates to S in $CS_2$, COS and IM8 in steps 1, 3 and 6, respectively), and intramolecular H migration (see steps 2, 4, 5 and 7). In steps 2, 5 and 7, the H in the OH group of the intermediate migrates to S, leading to the release of $H_2S$. It can be concluded that H migration plays an important role in $CS_2$ hydrolysis. However, it is difficult to determine which of the mechanisms is more favorable than the other from the microscopic structure. Therefore, analyses of the thermodynamic and kinetic functional changes during hydrolysis are needed.

## Thermodynamic analysis of $CS_2$ hydrolysis

The thermodynamic functional changes for the two mechanisms are listed in Table 3. In the two reaction pathways, the steps in which $H_2S$ is released via intramolecular H migration (steps 2, 5 and 7) have negative Gibbs free energy changes in Table 3, which shows that these steps are spontaneous processes under isothermal-isobaric conditions from a thermodynamic point of view. The steps involving the combination of two molecules—steps 1, 3 and 6—have positive Gibbs free energy changes, which shows that these steps are inhibited under isothermal-isobaric conditions. It can also be concluded that $CS_2$ hydrolysis is a feasible reaction from a thermodynamic point of view, as the total $\Delta_r S_m^{\circ}$ is positive and the total $\Delta_r G_m^{\circ}$ is negative, which means that it can occur at room temperature. However, despite the fact that hydrolysis of the $CS_2$ is thermodynamically feasible, the conversion rate within a certain time is low [29]. Kinetic data are therefore necessary to study the hydrolysis of $CS_2$ further.

## Kinetic analysis of $CS_2$ hydrolysis

A detailed kinetic analysis of the two mechanisms will be discussed in this section. According to transition state theory, the activation enthalpy $\Delta_r H_m^{\neq}$, activation entropy $\Delta_r S_m^{\neq}$ and activation energy $E_a$ can be obtained from Eqs. 3–5, respectively, while the rate constant $k$ can be expressed as in Eq. 6 [30, 31]:

$$\Delta_r H_m^{\neq} = H(TS) - H(R) \tag{3}$$

$$\Delta_r S_m^{\neq} = S(TS) - S(R) \tag{4}$$

$$E_a = \Delta_r H_m^{\neq} + nRT \tag{5}$$

**Table 3** The thermodynamic properties of $CS_2$ hydrolysis

| Steps | $\Delta_r H_m^\theta (\text{kJ} \cdot \text{mol}^{-1})$ | | $\Delta_r S_m^\theta (\text{J} \cdot \text{mol}^{-1} \cdot \text{K}^{-1})$ | | $\Delta_r G_m^\theta (\text{kJ} \cdot \text{mol}^{-1})$ | |
|---|---|---|---|---|---|---|
| | 298.15 K | 875 K | 298.15 K | 875 K | 298.15 K | 875 K |
| Two-step mechanism | | | | | | |
| Step 1 | 40.50 | 39.96 | −34.72 | −36.47 | 50.85 | 71.88 |
| Step 2 | −92.48 | −90.51 | 43.96 | 48.42 | −105.58 | −132.88 |
| Step 3 | −2.79 | −5.75 | −42.41 | −49.41 | 9.85 | 37.48 |
| Step 4 | 19.92 | 20.41 | 4.70 | 5.77 | 18.51 | 15.35 |
| Step 5 | −66.75 | −64.15 | 55.46 | 61.36 | −83.29 | −117.84 |
| One-step mechanism | | | | | | |
| Step 1 | 40.50 | 39.96 | −34.72 | −36.47 | 50.85 | 71.88 |
| Step 6 | 3.58 | 2.72 | −32.13 | −34.57 | 13.16 | 32.96 |
| Step 7 | −81.63 | −81.02 | 45.44 | 47.08 | −95.18 | −122.22 |
| Step 4 | 19.92 | 20.41 | 4.70 | 5.77 | 18.51 | 15.35 |
| Step 5 | −66.75 | −64.15 | 55.46 | 61.36 | −83.29 | −117.84 |
| Total | −110.10 | −110.97 | 20.10 | 17.45 | −116.10 | −126.26 |

$$k = \frac{k_b T}{h} \left( \frac{p^o}{RT} \right)^{1-n} \exp\left( \frac{-\Delta_r H_m^{\neq}}{RT} \right) \exp\left( \frac{\Delta_r S_m^{\neq}}{R} \right). \qquad (6)$$

Here, $k$ is the rate constant, $T$ is the reaction temperature, $k_b$, $h$, $p°$ and $R$ are Boltzmann's constant, Planck's constant, standard atmospheric pressure, and the fundamental gas constant, and $n$ is the number of reactants.

The activation parameters $\Delta_r H_m^{\neq}$, $\Delta_r S_m^{\neq}$, $E_a$, as well as the rate constant ln$k$ of every elementary reaction at the temperatures 298.15 K and 875 K, are shown in Table 4. According to the activation entropy ($\Delta_r S_m^{\neq}$) data in Table 4, it can be seen that these are entropy-decreasing pathways as the temperature increases. The activation enthalpy $\Delta_r H_m^{\neq}$ decreases slowly and monotonously with increasing temperature. We can also see that the activation energy of COS hydrolysis is lower than that of $CS_2$ hydrolysis, and the rate constant ln$k_1$ of step 1 is larger than the rate constant ln$k_3$ of step 3, which shows that $CS_2$ is more difficult than COS to hydrolyze, in agreement with the results of Huisman [7]. The activation energy of TS1 is the largest and the rate

**Table 4** The activation enthalpy, activation entropy, activation energy, and rate constant of each elementary reaction

| Elementary reaction | $\Delta_r H_m^{\neq}$ (kJ mol$^{-1}$) | | $\Delta_r S_m^{\neq}$ (J mol$^{-1}$ K$^{-1}$) | | $E_a$ (kJ mol$^{-1}$) | | ln$k$* | |
|---|---|---|---|---|---|---|---|---|
| | 298.15 K | 875 K | 298.15 K | 875 K | 298.15 K | 875 K | 298.15 K | 875 K |
| Two-step mechanism | | | | | | | | |
| Step 1 | 163.08 | 159.19 | −42.92 | −51.05 | 168.04 | 173.74 | −45.19 | −0.11 |
| Step 2 | 80.50 | 78.08 | 0.06 | −4.36 | 82.98 | 85.36 | −3.01 | 19.28 |
| Step 3 | 137.92 | 133.24 | −43.68 | −53.56 | 142.87 | 147.79 | −35.13 | 3.16 |
| Step 4 | 43.91 | 40.66 | −0.50 | −6.22 | 46.39 | 47.93 | 11.68 | 24.20 |
| Step 5 | 81.17 | 78.68 | −2.00 | −6.64 | 83.65 | 85.95 | −3.53 | 18.92 |
| One-step mechanism | | | | | | | | |
| Step 1 | 163.08 | 159.19 | −42.92 | −51.05 | 168.04 | 173.74 | −45.19 | −0.11 |
| Step 6 | 139.85 | 135.36 | −47.49 | −56.97 | 144.81 | 149.91 | −36.37 | 2.45 |
| Step 7 | 73.31 | 69.83 | −6.61 | −13.36 | 75.79 | 77.10 | −0.91 | 19.33 |
| Step 4 | 43.91 | 40.66 | −0.50 | −6.22 | 46.39 | 47.93 | 11.68 | 24.20 |
| Step 5 | 81.17 | 78.68 | −2.00 | −6.64 | 83.65 | 85.95 | −3.53 | 18.92 |

* Steps 1, 3 and 6 are second-order reactions: the units are mol$^{-1}$ dm$^3$ s$^{-1}$; steps 2, 4, 5 and 7 are first-order reactions: the units are s$^{-1}$

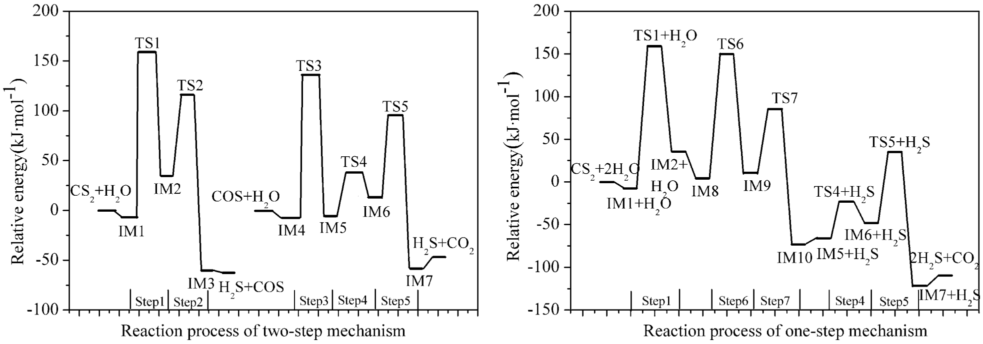

**Fig. 3** Sketch of the energies of the stationary points for $CS_2$ hydrolysis

constant $\ln k_1$ is the smallest in both mechanisms, which shows that step 1 (IM1→IM2) is the rate-determining step in both mechanisms. Although a higher barrier of 247.90 kJ $mol^{-1}$ to the proton transfer of $H_2O$ to $CS_2$ was obtained with the MP2 method by Deng et al. [21] compared to the value of 168.04 kJ $mol^{-1}$ obtained in our calculation, we reached the same conclusion: that the proton transfer process for the one-water hydrolysis mechanism of carbon disulfide is the rate-determining step. The energy barriers for the two mechanisms are similar, as shown in Fig. 3, which indicates that the two-step mechanism and the one-step mechanism are parallel and competitive. Increasing the reaction temperature favors $CS_2$ hydrolysis, as we can see by comparing to the rate constants at different temperatures in Table 4. However, the negative total $\Delta_r H°_m$ in Table 3 shows that $CS_2$ hydrolysis is an exothermic reaction, so increasing the temperature is disadvantageous for this reaction, in agreement with the results reported in [11]. So what is the optimal hydrolysis temperature of $CS_2$?

## The optimal hydrolysis temperature of $CS_2$

In order to find the optimal hydrolysis temperature of $CS_2$, the equilibrium constants lg$K$ and the rate constants ln$k$ of the rate-determining step at different temperatures are shown in Fig. 4 (these values can be obtained from Eqs. 7 [32] and 6), respectively. It is clear that the equilibrium constant lg$K$ decreases monotonously, and the rate constant ln$k$ of the rate-determining step increases monotonously with increasing hydrolysis temperature. There is a crossing point at about 525 K, which shows that the optimal temperature is about 252 °C when $CS_2$ hydrolysis is performed without catalysts. The hydrolysis temperature should be below 252 °C when a catalyst is used, and the precise temperature range varies depending on the catalyst, equipment, etc. used. Wang et al. [13] found that the conversion of $CS_2$ reaches 91% at 130 °C when the catalyst is 5% Ce, 14% $K_2CO_3$ and 81% $Al_{20}O_3$, the space velocity is 21773 $h^{-1}$, the relative humidity is 1.6%, and the $CS_2$ concentration is 160 mgS/$m^3$. However, $CS_2$ conversion in the presence of $Al_2O_3$ with 6% $K_2CO_3$ can reach more than 98% at 160 °C and atmospheric pressure when the space velocity is 10000 $h^{-1}$ [11].

$$\Delta_r G_m^\theta(T) = -RT \ln K^\theta \qquad (7)$$

## Conclusions

The process of $CS_2$ hydrolysis has been explored using density functional theory, and two detailed reaction mechanisms for $CS_2$ hydrolysis were presented. Ten intermediates and seven transition states occur along the reaction pathways. The results of a thermodynamic analysis show that $CS_2$ hydrolysis can occur at room temperature, but the reaction rate is very low. The rate-determining step of the two-step mechanism and one-step mechanism involves H and OH in $H_2O$ attacking S and C

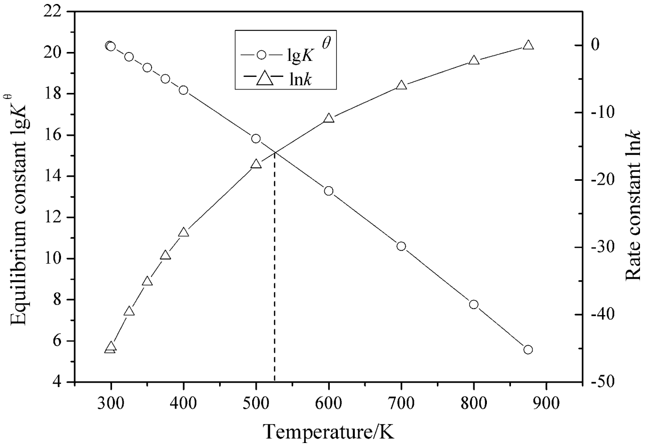

**Fig. 4** The equilibrium constant lg$K$ and the rate constant ln$k$ at different temperatures

in $CS_2$, respectively, so that the C=S double bond changes into a single bond. The two mechanisms are competitive. The optimal temperature is about 252 °C when $CS_2$ hydrolysis is performed without a catalyst, and the hydrolysis temperature should be below 252 °C when a catalyst is used.

**Acknowledgments** This work was supported by the National Natural Science Foundation of China (nos. 20776093, 20976115, 20906066), and the Foundation of Shanxi Province (no. 2009021015).

## References

1. Guo B, Chang LP, Xie KC (2006) Fuel Process Technol 87:873–881
2. Zou FL, Li CH, Guo HX (1997) J Mol Catal China 11:138–144
3. Yao XQ, Li YW (2009) J Mol Struct Theochem 899:32–41
4. Zhang RG, Ling LX, Wang BJ (2010) J Mol Model. doi:10.1007/s00894-010-0686-8
5. Shangguan J, Li CH, Guo HX (1998) J Nat Gas 7:24–30
6. Tong S, Dalla Lana IG, Chuang KT (1995) Can J Chem Eng 73:220–227
7. Huisman HM, van der Berg P, Mos R, van Dillen AJ, Geus JW (1994) Appl Catal A Gen 115:157–171
8. George ZM (1974) J Catal 32:261–271
9. Tong S, Dalla Lana IG, Chuang KT (1992) Can J Chem Eng 70:516–522
10. Wang L, Li FL, Wu DY, Wang SD, Yuan Q (2004) J Fuel Chem Technol 32:466–470
11. Zou FL, Li CH, Guo HX (1996) J Nat Gas 5:334–340
12. Shangguan J, Guo HX (1997) J Fuel Chem Technol 25:277–283
13. Wang L, Li FL, Wu DY, Wang SD, Yuan Q (2005) Nat Gas Chem Ind 30:1–5
14. Laperdrix E, Justin I, Costentin G, Saur O, Lavalley JC, Aboulayt A, Ray JL, Nédez C (1998) Appl Catal B Environ 17:167–173
15. Sahibed-Dine A, Aboulayt A, Bensitel M, Mohammed Saad AB, Daturi M, Lavalley JC (2000) J Mol Catal A Chem 162:125–134
16. Yang T, Wen XD, Huo CF, Li YW, Wang JG, Jiao HJ (2009) J Mol Catal A Chem 30:29–136
17. McKee ML (1993) Chem Phys Lett 201:41–46
18. Bohn RB, Brabson GD, Andrews L (1992) J Phys Chem 96:1582–1589
19. Wang YC, Lv LL, Dai GL, Wang DM, Geng ZY (2004) Chem Res 15:38–42
20. Zheng Y, Zhu YQ, Li LC (2005) J Sichuan Normal Univ (Nat Sci) 28:708–711
21. Deng C, Wu XP, Sun XM, Ren Y, Sheng YH (2009) J Comput Chem 30:285–294
22. Deng C, Li QG, Ren Y, Wong NB, Chu SY, Zhu HJ (2008) J Comput Chem 29:466–480
23. Delley B (2005) J Chem Phys 113:7756–7764
24. Perdew JP, Chevary JA, Vosko SH, Jackson KA, Pederson MP, Singh DJ, Fiolhais C (1992) Phys Rev B 46:6671–6687
25. Lide DR (2001) Handbook of chemistry and physics, 82nd edn. CRC, New York, pp 9-19–9-21
26. Ling LX, Zhang RG, Wang BJ, Xie KC (2009) J Mol Struct Theochem 905:8–12
27. Ling LX, Zhang RG, Wang BJ, Xie KC (2010) J Mol Struct Theochem 952:31–35
28. Ling LX, Zhang RG, Wang BJ, Xie KC (2009) Chin J Chem Eng 17:805–813
29. Rodes C, Riddel SA, West J, Williams BP, Hutchings GJ (2000) Catal Today 59:443–464
30. Hyre DE, Trong IL, Freitag S, Stenkamp RE, Stayton PS (2000) Protein Sci 9:878–885
31. Frisch C, Fersht AR, Schreiber G (2001) J Mol Biol 308:69–77
32. Fu XC, Shen WX, Yao TY (1990) Physical chemistry, 4th edn. Higher Education Press, Beijing, p 387